IEEE Access
Multidisciplinary ⋮ Rapid Review ⋮ Open Access Journal

Received December 25, 2021, accepted January 12, 2022, date of publication January 14, 2022, date of current version January 27, 2022.

Digital Object Identifier 10.1109/ACCESS.2022.3143577

BA-Based Low-PSLL Beampattern Synthesis in the Presence of Array Errors

ANYI WANG, XUHONG LI, AND YANHONG XU, (Member, IEEE)
School of Communication and Information Engineering, Xi'an University of Science and Technology, Xi'an 710054, China

Corresponding author: Yanhong Xu (yanhongxuxidian@163.com)

This work was supported in part by the Natural Science Foundation of China (NSFC) under Grant 61901357 and Grant U19B2015, and in part by the National Key Research and Development Plan Internet more than Coal Mine Safety Supervision and Monitoring Key Technology Development and Demonstration under Grant 2018YFC0808301.

ABSTRACT In practical scenarios, there are always array errors, which would increase the sidelobe level (SLL) of the array and distort the performance of the electronic devices consequently. Nevertheless, most of the reported works do not take these unavoidable errors into consideration when implementing array beampattern synthesis. To remedy this problem, a low sidelobe beampattern synthesis approach is proposed in the presence of array errors based on the bat algorithm (BA). In particular, the covariance matrix of the sidelobe region in the presence of array errors is incorporated into the optimization problem. Generally, there are many factors that would contribute to array errors in practical scenarios. Therefore, to reduce the influence of the uncertainty characteristic of the errors on the low-SLL beampattern synthesis, the statistical mean method is utilized to obtain a robust calculation of the covariance matrix in the presence of array errors. Theoretical analysis using signal processing technique and electromagnetic simulation using Ansoft HFSS workbench are combined to testify the effectiveness of the proposed approach. Numerical results show that peak SLLs (PSLLs) of around −22dB and −20dB can be respectively achieved in the above two simulation situations with the obtained weight vectors.

INDEX TERMS Pattern synthesis, array errors, low sidelobe level, covariance matrix, bat algorithm.

I. INTRODUCTION

Low-sidelobe beampattern synthesis is one of the most important issues in array antenna synthesis since it can reduce the energy leakage in the region out-of-interest, thus improving the array energy efficiency and reducing the influence of the interferences and/or clutter on the array performance in sidelobe-region simultaneously [1], [2]. Typical amplitude tapering methods were firstly proposed to reduce the sidelobe level (SLL) of the array, such as Chebyshev distribution [3], Taylor distribution [4], Gaussian distribution [5], and hybrid distribution [6]. In general, not only the array amplitudes, but also the phases and positions of the elements in an array can be properly adjusted to achieve low SLL [7]. A series of global optimization methods, such as particle swarm optimization (PSO) algorithm [8], genetic algorithm (GA) [9], hybrid algorithm [10], and *et. al.*, have been proposed to obtain complex exciting weight values of the elements for low SLL array design. A pencil beam in the broadside direction is produced with low SLL by iteratively modifying the positions of the elements [11].

In practical scenarios, array errors always exist unavoidably due to many factors, such as element position errors, mutual coupling effects among elements, amplitude and phase errors of exciting currents, which would increase the SLL and distort the performance of the electronic devices consequently. At present, some types of array errors have been taken into consideration when implementing relative research. In [12], an interval analysis method accompanied by convex programming was proposed to design robust beamformer weights for array antennas with amplitude errors. In [13], a novel matrix-based interval arithmetic method was proposed for linear antenna array pattern tolerance analysis with excitation amplitude errors. The iterative Fourier transform technique was utilized to mitigate the degradation of sidelobe performance of array antenna caused by quantization of its taper across the array in [14]. In [15], the differential evolution (DE) algorithm was adopted to synthesize array

The associate editor coordinating the review of this manuscript and approving it for publication was Giorgio Montisci.

antenna for microwave power transmission with excitation errors taken into consideration. In [16], a conical method was proposed for the representation of position errors by considering both the relevance and the randomness of the adjacent planar array elements. In [17], Schmid presented the worst-case boundaries and a statistical analysis of the beampattern deviation for linear, angle-independent calibration error and mutual coupling models. However, it is found that most of the state-of-the-art works only consider one or two factors that contribute(s) to array errors after a thorough literature review.

Inspired by the echolocation behavior of bats, Dr. Yang proposed a new metaheuristic algorithm [18], i.e., the bat algorithm (BA), in 2010. It has been demonstrated that this algorithm is a powerful optimization algorithm, which is superior to the famous standard PSO and GA in terms of accuracy and efficiency [18], [19]. Since then, the BA has been applied in some engineering applications including the array beamforming [19]–[22] and antenna design [23]. Nevertheless, the applications of this algorithm in antenna field is quite limited. Under this circumstance, we aim to propose an efficient low-PSLL beampattern synthesis approach in the presence of array errors based on this algorithm to utilize its excellent performance. A more general array error model established in [24] is adopted during the low-PSLL optimization procedure, where the above mentioned errors are boiled down to the amplitude and phase response errors. Meanwhile, the covariance matrix of the sidelobe region is incorporated into the optimization problem. To reduce the influence of the uncertainty characteristic of the errors, the statistical mean method is utilized to obtain a more robust calculation of the covariance matrix in the presence of array errors. Both of the theoretical analysis using signal processing technique and electromagnetic simulation using Ansoft HFSS workbench are adopted to testify the effectiveness of the proposed approach.

The remainder of this paper is organized as follows. Section II firstly formulates the signal model of the problem. On this basis, Section III derives the proposed low-PSLL beampatten synthesis approach in the presence of array errors based on BA. Numerical results are presented in Section IV to demonstrate the effectiveness of the proposed approach, and the conclusion is drawn in Section V.

II. PROBLEM FORMULATION

As depicted in Fig. 1., consider a uniform linear array (ULA) consisting of M elements, the inter-element spacing of which is d. Taking the first element of the ULA as the reference point, the steering vector of the array can be written as [25]

$$\mathbf{a}(\theta) = \left[e^{j\vec{k}\cdot\vec{x}_1}, \cdots, e^{j\vec{k}\cdot\vec{x}_m}, \cdots, e^{j\vec{k}\cdot\vec{x}_M}\right]^{\mathrm{T}} \tag{1}$$

where $\mathbf{a}(\theta) \in \mathbb{C}^{M\times 1}$, the superscript $^{\mathrm{T}}$ denotes the transpose operator, $\vec{k} = 2\pi/\lambda\,[\sin(\theta), \cos(\theta)]^{\mathrm{T}}$ stands for the wave vector with λ being the operational wavelength, θ is defined as the angle deviating from the positive y-axis. $\vec{x}_m = [(m-1)\,d, 0]^{\mathrm{T}}$, $m = 1, \cdots, M$ is the position vector of the mth element. Then the beampattern of the array can be expressed as

$$P(\theta) = \left|\mathbf{w}^{\mathrm{H}}\mathbf{a}(\theta)\right|^2 = \mathbf{w}^{\mathrm{H}}\mathbf{R}(\theta)\,\mathbf{w} \tag{2}$$

where $\mathbf{w} \in \mathbb{C}^{M\times 1}$ denotes the array weight vector, the superscript $^{\mathrm{H}}$ denotes the conjugate transpose operator, and $\mathbf{R}(\theta) = \mathbf{a}(\theta)\,\mathbf{a}^{\mathrm{H}}(\theta) \in \mathbb{C}^{M\times M}$ is the covariance matrix of the array. Nevertheless, in practical scenario, $\mathbf{a}(\theta)$ cannot be directly utilized to calculate $\mathbf{R}(\theta)$ due to the existence of the array errors. To alleviate this problem, an effective approach is to adopt the steering vector in the presence of array errors instead of the ideal one when calculating the covariance matrix of the array.

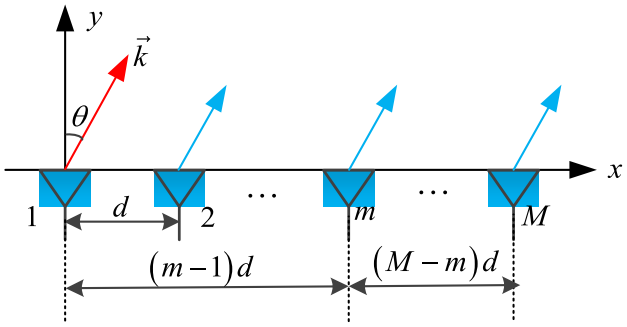

FIGURE 1. Configuration of a ULA.

In the following, a more general array error model is established. It is known that the amplitude and phase responses are two key parameters that play quite important roles in array beamforming [25]. When these two factors are determined, the beampattern of the array is determined. In practical scenario, there exist many kinds of array errors and these errors always occur simultaneously. Thus, it is unreal to separate a specific kind of array error and explore its effect on the array beampattern. All these array errors have influences on the amplitude and phase responses, which causes the array beampattern error. Therefore, it is reasonable that the influence of these errors on the array beampattern are boiled down to the amplitude and phase response errors [24]. In specific, the array error vector can be expressed as

$$\mathbf{e} = [e_1, \cdots, e_m, \cdots, e_M]^{\mathrm{T}} \tag{3}$$

where $e_m = (1+\alpha_m)\,e^{j\beta_m}$ denotes the response error of the mth element with α_m and β_m being the amplitude and the phase parts of the error, and respectively satisfying the Gaussian random distribution and zero mean uniformly random distribution.

In this case, the beampattern of the array in the presence of array errors can be reconstructed as

$$P_e(\theta) = \mathbf{w}^{\mathrm{H}}\mathbf{R}_e(\theta)\,\mathbf{w} \tag{4}$$

where $\mathbf{R}_e(\theta) = \mathbf{a}_e(\theta)\,\mathbf{a}_e^{\mathrm{H}}(\theta)$, and $\mathbf{a}_e(\theta) = \mathbf{e}\odot\mathbf{a}(\theta)$ denotes the array steering vector in the presence of array errors

where $\odot$ stands for the Schur-Hadamard product. These errors would drastically increase the SLL of the array and distort the performance of the array correspondingly. As an illustration, Fig. 2 presents four normalized array patterns, i.e., pattern 1: the ideal one generated with uniform weight vector; pattern 2: the pattern generated with uniform weight vector in the presence of array errors; pattern 3: the ideal one generated with -20dB Chebyshev window; and pattern 4: the pattern generated with -20dB Chebyshev window in the presence of array errors. From Fig. 2, it can be seen that the PSLLs of the array are increased by 4.2dB (from -13.2dB to -9.0dB) and 6.5dB (from -20.0dB to -13.5dB) when utilizing the uniform weight vector and -20 Chebyshev tapering vector, respectively, in the presence of 10% errors. Note that the specific increased value is not a fixed number since the errors cannot be determined. Herein, Fig. 2 is utilized to demonstrate that large SLL increment would appear in case of array errors.

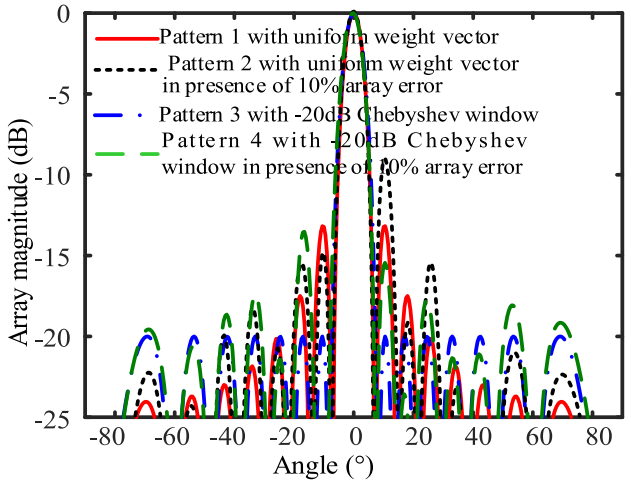

FIGURE 2. Normalized array beampatterns with and without array errors, where the array errors of 10% are taken into consideration. In particular, a half-wavelength spaced 16-element linear array is considered, where $f = 8$GHz.

III. THE PROPOSED LOW-SIDELOBE BEAMPATTERN SYNTHESIS APPROACH IN THE PRESENCE OF ARRAY ERRORS

The aim of this section is to find the optimal complex-valued weight vector $\mathbf{w}$ which can minimize the maximum power from the sidelobe region subject to a distortionless constraint for a specified steering vector of interest in the presence of array errors. In particular, the covariance matrix $\mathbf{R}_e(\theta)$ of the sidelobe region is incorporated into the optimization problem. As has been pointed out in Section II, the induced amplitude and phase response errors of the array comply with random distribution. Therefore, to reduce the influence of the uncertainty characteristic of the errors on the low-SLL beampattern synthesis, the statistical mean method is utilized to obtain a more robust calculation of the covariance matrix of the sidelobe region in the presence of array errors.

Executing L Monte Carlo trials, the mean value of the covariance matrix $\mathbf{R}_e(\theta)$ in the presence of array errors can be expressed as

$$\hat{\mathbf{R}}_e(\theta) = \frac{1}{L}\sum_{l=1}^{L}\mathbf{R}_e^l(\theta) \tag{5}$$

where $\theta \in \left[-\frac{\pi}{2}, \theta_1\right) \cup \left(\theta_2, \frac{\pi}{2}\right]$ denotes the sidelobe region of the array with θ_1 and θ_2 ($\theta_1 < \theta_2$) being the two edge points of the sidelobe region. $\mathbf{R}_e^l(\theta)$ is the covariance matrix of the sidelobe region generated in the lth Monte Carlo trial with array errors taken into consideration. Therefore, the optimization problem to be solved can be constructed as

$$\min_{\mathbf{w}} \mathbf{w}^{\mathrm{H}}\hat{\mathbf{R}}_e(\theta)\,\mathbf{w}, \tag{6}$$

subject to

$$P_g(\theta)\big|_{\theta=\theta_0} = 1, \tag{7a}$$

and

$$P_g(\theta)\big|_{\theta=\theta_1} = P_g(\theta)\big|_{\theta=\theta_2} = 0 \tag{7b}$$

where $P_g(\theta)$ denotes the generated pattern in the presence of array errors. Specifically, Eq. (7a) is utilized to guarantee that the mainbeam of the generated beampattern is steered to the desired direction θ_0, and Eq. (7b) provides the constraints imposed on the mainbeam width which is $\theta_2 - \theta_1$.

In this way, the fitness function can be represented as

$$f(\mathbf{w}) = \min_{\mathbf{w}} \max_{\theta\in[-\frac{\pi}{2},\theta_1)\cup(\theta_2,\frac{\pi}{2}]} \mathbf{w}^{\mathrm{H}}\hat{\mathbf{R}}_e(\theta)\,\mathbf{w} \tag{8}$$

which is decreased as the weight vector $\mathbf{w}$, i.e., the position of bat in BA, updated iteratively. It is noted that the PSLL and integrated SLL are the two main metrics for evaluating the array beampattern. Actually, if the PSLL of the beampattern is well controlled, the integrated SLL can also be controlled. Herein, we only consider the PSLL and do not incorporate the integrated SLL.

In the sequel, we define the rule how the position $\mathbf{w}_i$ and velocity $\mathbf{v}_i$ of the ith bat in BA are updated in a $2M$-dimensional (including the real and imaginary parts of the weight vector) search space. The new solution $\mathbf{w}_{i+1}$ and velocities $\mathbf{v}_{i+1}$ at time $t+1$ are obtained by

$$F_i = F_{\min} + (F_{\max} - F_{\min})\,\beta, \tag{9a}$$

$$\mathbf{v}_i^{t+1} = \mathbf{v}_i^t + F_i\left(\mathbf{w}_i^t - \mathbf{w}_g^t\right), \tag{9b}$$

and

$$\mathbf{w}_i^{t+1} = \mathbf{w}_i^t + \mathbf{v}_i^{t+1}, \tag{9c}$$

where $\mathbf{w}_g^t$ represents the global best position of all the bats at time step t iteration, $F_{\min}$, $F_{\max}$ and β are system parameters that controls the algorithm performance. It is seen from Eq. (9) that, the velocity is utilized to update the position of the bat. As the iteration proceeds, $\mathbf{v}_i^{t+1}$ is utilized to update $\mathbf{w}_i^t$ to $\mathbf{w}_i^{t+1}$ after evaluation. It defines how the position vector is updated. Usually, $F_{\min} = 0$, $F_{\max} = 2$, and $\beta \in [0, 1]$

is a uniform distributed random variable for beamforming applications.

In nature, bats utilize the ultrasonic wave to find preys. When a bat has found its prey, the loudness of the ultrasonic wave decreases and the rate of pulse emission increases. Therefore, two more judgement parameters are introduced in BA, i.e., the rate r_i and the loudness A_i. It should be highlight that these two parameters will be updated only if the new solutions are improved, which means that these bats are moving towards the optimal solution. In specific, their loudness and emission rates will be updated in the following way

$$r_i^{t+1} = r_i^1 \left[1 - \exp\left(-\zeta t\right)\right], \tag{10a}$$

and

$$A_i^{t+1} = \xi A_i^t, \tag{10b}$$

where $\zeta > 0$ and $0 < \xi < 1$ are constants to guarantee $\lim_{t\to\infty} r_i = r_i^1$ and $\lim_{t\to\infty} A_i = 0$ which indicates that a solution is just found and the iteration is stopped. Initially, each bat should have different values of loudness and pulse emission rate, and this can be achieved by randomization. For example, the initial loudness A_i^1 can typically be [1, 2], while the initial emission rate r_i^1 can be around zero, or any value $r_i^1 \in [0, 1]$.

Algorithm 1 Pseudo Code of the BA-Based Low-SLL Optimization Algorithm

1) Initialize $\mathbf{w}_i$, $\mathbf{v}_i$, r_i, A_i, and N_{iter};
2) Calculate $f(\mathbf{w}_i)$ according to Eq. (8), find the best solution $\mathbf{w}_g$ and the minimum $f(\mathbf{w}_g)$;
3) **While** ($t < N_{\text{iter}}$)
  Initialize F_i, and update $\mathbf{w}_i$ and $\mathbf{v}_i$ according to Eq. (9);
  if ($rand > r_i$)
    $\mathbf{w}_i = \mathbf{w}_g + \gamma \text{randn}(2M, 1)$
  end if
  if ($rand < A_i$ and $f(\mathbf{w}_i) < f(\mathbf{w}_g)$)
    Accept the new solutions;
    Update $\mathbf{w}_g$ and $f(\mathbf{w}_g)$;
    Increase r_i and reduce A_i;
  end if
 end while

Output: $\mathbf{w}_{\text{opt}} = \mathbf{w}_g$ and $f(\mathbf{w}_g)$

To be more specific, Algorithm 1 provides the pseudo code of the BA-based optimization algorithm, where N_{iter} denotes the max number of iterations and $\gamma \in [-1, 1]$ is a randomly walking parameter. Note that a preliminary evaluation of the positions initialized in step 1 is performed in step 2. As an illustration, when evaluating the position of the ith bat, i.e., $\mathbf{w}_i$, calculate $\mathbf{w}_i^{\text{H}} \hat{\mathbf{R}}_e(\theta) \mathbf{w}_i$ and find its maximum value in the sidelobe region, i.e., $[-\pi/2, \theta_1) \cup (\theta_2, \pi/2]$. Note that the mainlobe region $[\theta_1, \theta_2]$ is predesigned. Theoretically, it can be set as any value, which is not less than the counterpart of the array generated with uniform weight vector in ideal scenario. After calculating the positions of all bats, find the minimum one among all of the maximum values. Then, set the position of the bat, which can generate the minimum value, as the best solution $\mathbf{w}_g$, and record the minimum value as $f(\mathbf{w}_g)$ in this current iteration. From this algorithm, it is seen that an optimal weight vector $\mathbf{w}_{\text{opt}}$ is obtained after the optimization.

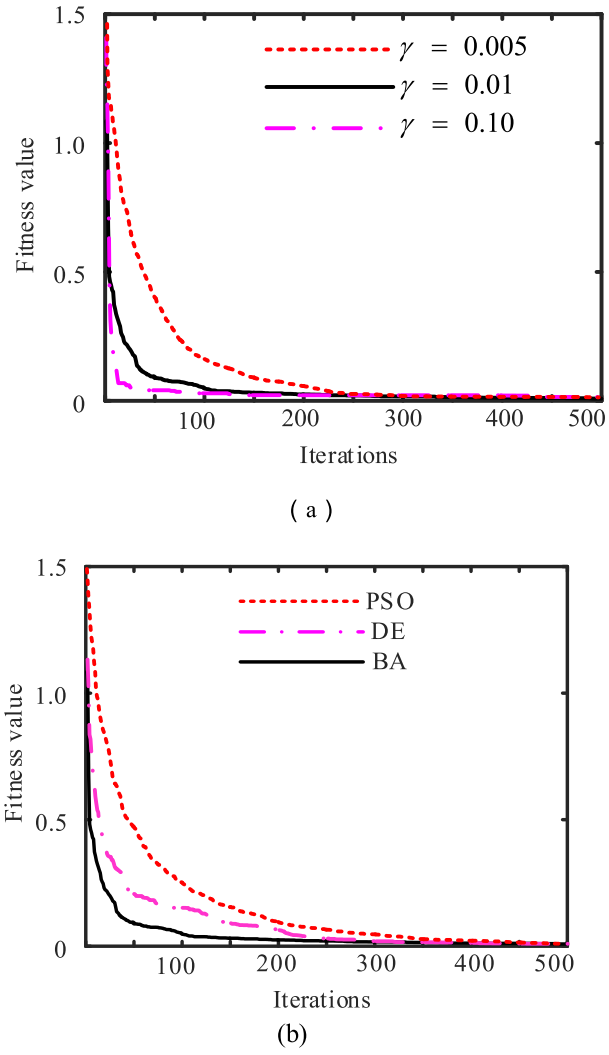

FIGURE 3. Convergence curves of the fitness value versus the number of iterations. (a) Different γ values. (b) Different algorithms under the same situation.

TABLE 1. Simulated parameters.

Parameters	Values	Parameters	Values	Parameters	Values
M	16	f	8GHz	ζ	0.8
d	$0.5\lambda_0$	L	200	ξ	0.8
γ	0.01	N_{iter}	500		

Hence, the resultant low-SLL beampattern of the array can be represented as

$$\hat{\text{P}}_g(\theta) = \mathbf{w}_{\text{opt}}^{\text{H}} R_e(\theta) \mathbf{w}_{\text{opt}}. \tag{11}$$

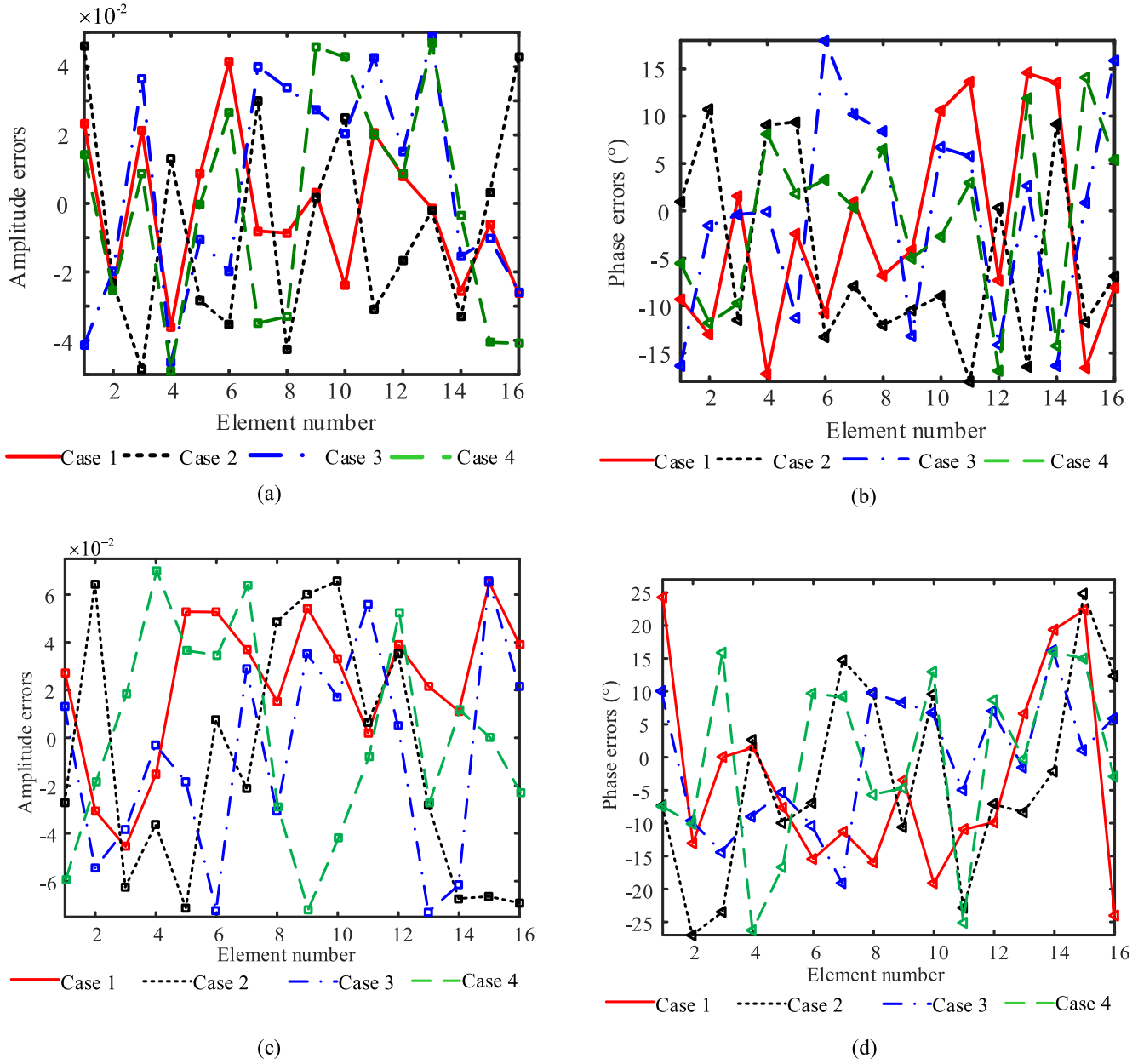

FIGURE 4. Four sets of randomly generated array errors. (a) Amplitude part and (b) Phase part of the 10% error. (c) Amplitude part and (d) Phase part of the 15% error.

Note that $R_e(\theta)$ is the covariance matrix under a certain random array error. Since $\mathbf{w}_{\text{opt}}$ is obtained with $\hat{\mathbf{R}}_e(\theta)$, it is robust against array errors in low-PSLL beamforming.

IV. NUMERICAL RESULTS

In this section, numerical results including the results generated with signal processing method and those obtained using Ansoft HFSS workbench are provided to investigate the effectiveness of the proposed approach in the presence of array errors. Table 1 provides the corresponding simulated parameters. As depicted in Eq. (10), for any $\zeta > 0$ and $0 < \xi < 1$, $\lim_{t\to\infty} r_i = r_i^1$ and $\lim_{t\to\infty} A_i = 0$ can be guaranteed. For the simplicity case, we set $\zeta = \xi = 0.8$. Meanwhile, as the beamwidth of the 16-element linear array is 16° in ideal scenario with uniform weight vector, $\theta_2 - \theta_1$ is set as 20° in the following simulations as an illustration to demonstrate the effectiveness of the proposed approach.

Firstly, we investigate the influence of the walking parameter γ on the convergence performance of the optimization approach. The convergence curves when $\gamma = 0.005$, $\gamma = 0.01$ and $\gamma = 0.1$ are provided in Fig. 3(a), from which it can be seen that the fitness values of the proposed optimization approach drops faster with the increment of γ. Finally, we set $\gamma = 0.01$ for a moderate convergence of the algorithm.

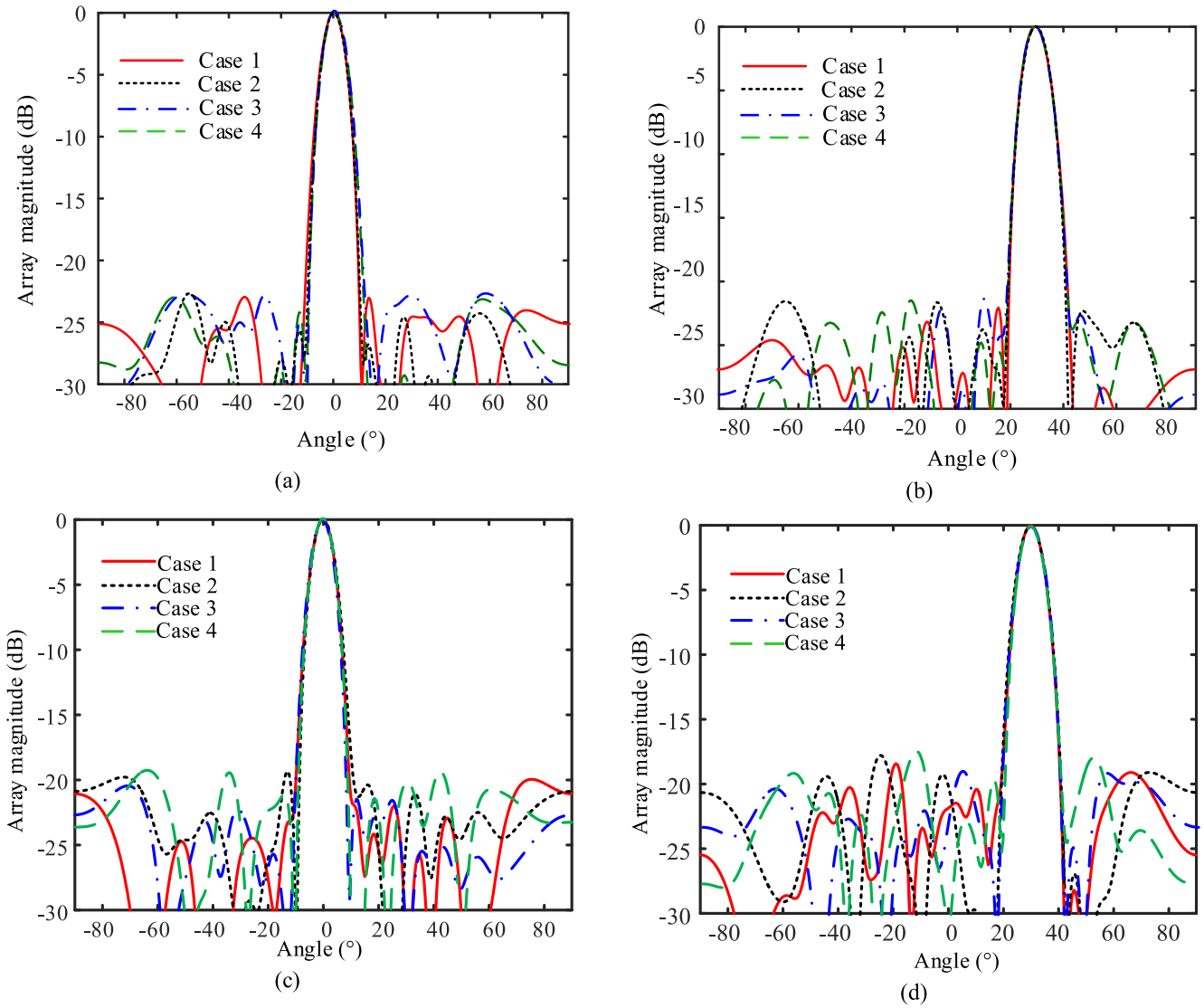

FIGURE 5. The normalized array pattern in the above four cases after utilizing the obtained optimized weight vector. (a) and (b) respectively correspond to $\theta_0 = 0°$ and $\theta_0 = 30°$ for 10% array error. (c) and (d) correspond to $\theta_0 = 0°$ and $\theta_0 = 30°$ for 15% array error.

In Fig. 3(b), we explore the convergence of the proposed algorithm as well as the PSO and DE algorithms. It is seen that the BA-based algorithm has higher efficiency compared with the state-of-the-art heuristic algorithms. The reason is that BA optimization adjust its parameters within the algorithms itself, which accelerates the convergence of the algorithm.

As described in Section III, the statistical mean method is adopted when calculating the covariance matrix of the sidelobe region. In this Section, two situations, i.e., the beam steered to 0° and 30°, are considered. The accordingly amplitude and phase parts of the generated optimal weight vectors in these two situations are provided in Tables 2-3.

To demonstrate the robustness of the obtained $\mathbf{w}_{\text{opt}}$ in low-SLL beampattern synthesis, we adopt four sets of randomly generated errors cases, i.e., Case 1, Case 2, Case 3 and Case 4, respectively under the array error of 10% and 15%. The amplitude and phase parts of these four sets of errors are provided in Fig. 4. In Figs. 4(a) and (b), it is seen that the magnitude error is randomly distributed within $[-5\%, 5\%]$ while the phase error is randomly distributed within $[-18°, 18°]$. In Figs. 4(c) and (d), the magnitude error belongs to $[-7.5\%, 7.5\%]$ while the phase error is within $[-27°, 27°]$. In practice, the array error can be smaller than that considered in this example. It is possible to adjust the array error based on the experimental results. The proposed algorithm is feasible for a relatively wide range of the array error.

Fig. 5 provides the corresponding normalized array patterns in these four cases after applying the obtained weight vectors $\mathbf{w}_{\text{opt}}$ when the beam is steered to 0° and 30° at the array error of 10% and 15%, respectively. As can be seen from Figs. 5(a) and (b), the generated PSLLs are all around -23.0dB and -21.5dB, respectively, for $\theta_0 = 0°$ and $\theta_0 = 30°$ when exists 10% array error. As the errors in these four cases are different from each other, it can be concluded

TABLE 2. The amplitude and phase parts of the optimized weight vector $\mathbf{w}_{opt}$ when there exist 10% array error.

Element number	Amplitude		Phase (°)	
	θ_0=0°	θ_0=30°	θ_0=0°	θ_0=30°
1	0.122	0.202	5.1	44.0
2	0.225	0.299	5.3	323.6
3	0.345	0.425	4.9	237.8
4	0.491	0.588	2.1	151.7
5	0.622	0.714	6.3	59.9
6	0.765	0.836	5.9	329.0
7	0.860	0.915	2.6	243.2
8	0.959	0.992	2.0	154.9
9	1.000	1.000	3.9	66.3
10	0.973	0.933	2.8	339.0
11	0.869	0.836	3.4	248.7
12	0.755	0.713	3.3	160.1
13	0.603	0.581	4.1	71.6
14	0.462	0.433	2.1	341.8
15	0.325	0.290	0.2	258.4
16	0.175	0.213	0.0	178.4

TABLE 3. The amplitude and phase parts of the optimized weight vector $\mathbf{w}_{opt}$ when there exist 15% array error.

Element number	Amplitude		Phase (°)	
	θ_0=0°	θ_0=30°	θ_0=0°	θ_0=30°
1	0.223	0.456	6.6	68.2
2	0.295	0.517	7.1	165.8
3	0.408	0.625	12.8	247.1
4	0.584	0.770	5.0	340.8
5	0.659	0.900	3.1	61.8
6	0.815	0.945	6.4	155.3
7	0.916	1.000	2.5	245.2
8	1.000	0.962	7.8	334.2
9	0.934	0.929	4.8	59.6
10	0.938	0.849	4.9	151.1
11	0.867	0.690	8.4	244.2
12	0.787	0.559	6.2	328.9
13	0.633	0.381	2.8	66.5
14	0.504	0.316	11.5	150.2
15	0.325	0.140	4.7	242.7
16	0.352	0.126	0.0	332.6

TABLE 4. The PSLLs of the four cases when 10% array error exists after the optimization.

Case 1 (dB)		Case 2(dB)	
θ_0=0°	θ_0=30°	θ_0=0°	θ_0=30°
-23.3	-21.8	-23.1	-21.3
Case 3(dB)		Case 4(dB)	
θ_0=0°	θ_0=30°	θ_0=0°	θ_0=30°
-22.7	-21.2	-22.8	-21.4

that the obtained weight vector is robust against the array error, which in turn demonstrates the effectiveness of the proposed approach. Besides, it is seen that the available PSLL is increased with respect to the increment of steered angle. Table 4 presents the specific PSLLs of the generated patterns in these four cases after applying the proposed approach. As comparison, the beampatterns are plotted for the 15% array error in Figs. 5(c) and (d). It is seen that the PSLLs of the beampattern are slightly higher. In the simulation example, it becomes −19.0dB for steered angle 0° while −17.4dB for steered angle 30°. Nevertheless, the proposed algorithm is still effective for this increased array error situation.

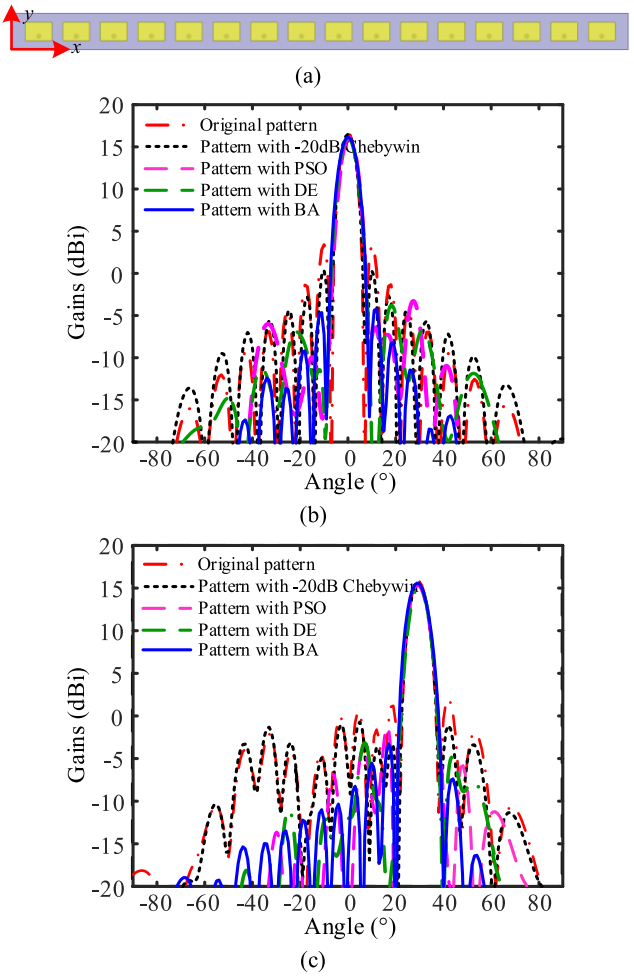

FIGURE 6. (a) Geometry of the half-wavelength spaced 16-element microstrip array antenna. (b) Patterns of the microstrip array antenna when beam is steered to 0°. (c) Patterns of the microstrip array antenna when beam is steered to 30°.

Mutual coupling effect among elements is unavoidable in practical scenario, which is a common factor that can cause large array errors. The existence of mutual coupling effect would increase the SLL of the array and distort the performance of the array accordingly. To further check the effectiveness of the proposed approach, electromagnetic simulation results using Ansoft HFSS workbench are provided. Specifically, a 16-element microstrip array antenna is designed, the mutual coupling of which is around −13.5dB among two adjacent elements. Figs. 6 (b)-(c) present the patterns after applying the obtained weights. The original patterns and the patterns applied with −20dB Chebywin weights are also provided as comparison. In particular, the original patterns are provided to show the original PSLLs of the array before implementing the low-PSLL beampattern synthesis. The patterns applied with −20dB Chebywin weights are provided

TABLE 5. The PSLLs of the four cases when 15% array error exists after the optimization.

Case 1 (dB)		Case 2(dB)	
θ_0=0°	θ_0=30°	θ_0=0°	θ_0=30°
-20.1	-18.4	-19.4	-17.7
Case 3(dB)		Case 4(dB)	
θ_0=0°	θ_0=30°	θ_0=0°	θ_0=30°
-20.5	-19.0	-19.0	-17.4

TABLE 6. The PSLLs of the patterns provided in Fig. 6.

θ_0=0° (dB)				
Orig	Cheby	PSO	DE	BA
-13.3	-16.1	-20.0	-20.5	-20.8
θ_0=30° (dB)				
Orig	Cheby	PSO	DE	BA
-13.0	-15.0	-16.7	-18.3	-18.5

to show the obtained PSLLs of amplitude tapering method when the mutual coupling exists. It is known that the beampattern generated with Chebyshev tapering weight vector has equal sidelobe levels without taking the element pattern into consideration. The resultant beampattern of the array is the product of the array pattern and the element pattern. The element pattern exhibit the property that its sidelobes level decrease as the sidelobe grow farther away from the mainlobe. Namely, the resultant beampattern can be viewed as the weighted array pattern, where the element pattern acts as the weight. Therefore, the black curve sidelobes level decrease as the sidelobe grow farther away from the mainlobe. It is seen from Figs. 6(b) and (c) that the PSLLs of -16.1dB and -15.0dB are achieved, respectively, for $\theta_0 = 0°$ and $\theta_0 = 30°$ after applying the -20dB Chebywin weights, while the PSLLs of -20.8dB and -18.5dB are obtained with the proposed approach. Besides, we also testify other heuristic optimization algorithms in this experiment, including PSO and DE algorithms. It is seen that the proposed BA-based algorithm performs slightly better than the PSO and DE algorithms. Namely, the proposed approach is still effective when strong mutual coupling effects exist. The specific PSLLs of the patterns in Figs. 6(b)-(c) are provided in Table 6. From Fig. 6, it is seen that with the increment of θ_0, the PSLLs are increased in both situations. It is also observed that we can draw the same conclusion with beapatterns pointing towards 0° and 30°. Besides, we find that the proposed approach is feasible for the beampatterns with beam steering direction within $-30° \sim 30°$. At present, the RF circuit design for the array still needs more efforts at present. Therefore, we plan to build the linear array as well as the corresponding RF circuit to further test the performance of the array in the near future.

V. CONCLUSION

In this paper, an effective beampattern synthesis approach is proposed to achieve low PSLL in the presence of errors based on the advanced BA. In specific, the covariance matrix in the presence of array errors is incorporated into the optimization problem. Meanwhile, the statistical mean method is utilized to obtain a robust calculation of the covariance matrix. Numerical results show that the proposed approach is superior over PSO and DE algorithms in terms of convergence rate and the performance of the obtained array pattern.

REFERENCES

[1] R. C. Hansen, *Phased Array Antennas*. Hoboken, NJ, USA: Wiley, 2009.
[2] W. L. Stutzman and G. A. Thiele, *Antenna Theory and Design*, 3rd ed. Hoboken, NJ, USA: Wiley, 2013.
[3] A. Koretz and B. Rafaely, "Dolph–Chebyshev beampattern design for spherical arrays," *IEEE Trans. Signal Process.*, vol. 57, no. 6, pp. 2417–2420, Jun. 2009.
[4] A. F. Morabito, "Synthesis of maximum-efficiency beam arrays via convex programming and compressive sensing," *IEEE Antennas Wireless Propag. Lett.*, vol. 16, pp. 2404–2407, 2017.
[5] G. Buttazzoni and R. Vescovo, "Density tapering of linear arrays radiating pencil beams: A new extremely fast Gaussian approach," *IEEE Trans. Antennas Propag.*, vol. 65, no. 12, pp. 7372–7377, Dec. 2017.
[6] B. Q. You, L. R. Cai, J. H. Zhou, and H. T. Chou, "Hybrid approach for the synthesis of unequally spaced array antennas with sidelobes reduction," *IEEE Antennas Wireless Propag. Lett.*, vol. 14, pp. 1569–1572, 2015.
[7] R. J. Mailloux, *Phased Array Antenna Handbook*. Boston, MA, USA: Artech House, 2005.
[8] S. K. Goudos, V. Moysiadou, T. Samaras, K. Siakavara, and J. N. Sahalos, "Application of a comprehensive learning particle swarm optimizer to unequally spaced linear array synthesis with sidelobe level suppression and null control," *IEEE Antennas Wireless Propag. Lett.*, vol. 9, pp. 125–129, 2010.
[9] G. Oliveri and A. Massa, "Genetic algorithm (GA)-enhanced almost difference set (ADS)-based approach for array thinning," *IET Microw., Antennas Propag.*, vol. 5, no. 3, pp. 305–315, Feb. 2011.
[10] C. Cui, W. T. Li, X. T. Ye, and X. W. Shi, "Hybrid genetic algorithm and modified iterative Fourier transform algorithm for large thinned array synthesis," *IEEE Antennas Wireless Propag. Lett.*, vol. 16, pp. 2150–2154, 2017.
[11] G. Buttazzoni and R. Vecovo, "Reducing the sidelobe power pattern of linear broadside arrays by refining the element positions," *IEEE Antennas Wireless Propag. Lett.*, vol. 17, no. 8, pp. 1464–1468, Aug. 2018.
[12] P. Rocca, N. Anselmi, and A. Massa, "Optimal synthesis of robust beamformer weights exploiting interval analysis and convex optimization," *IEEE Trans. Antennas Propag.*, vol. 62, no. 7, pp. 3603–3612, Jul. 2014.
[13] G. He, X. Gao, and H. Zhou, "Matrix-based interval arithmetic for linear array tolerance analysis with excitation amplitude errors," *IEEE Trans. Antennas Propag.*, vol. 67, no. 5, pp. 3516–3520, May 2019.
[14] W. P. M. N. Keizer, "Low sidelobe phased array pattern synthesis with compensation for errors due to quantized tapering," *IEEE Trans. Antennas Propag.*, vol. 59, no. 12, pp. 4520–4524, Dec. 2011.
[15] H.-W. Zhou, X.-X. Yang, and S. Rahim, "Array synthesis for optimal microwave power transmission in the presence of excitation errors," *IEEE Access*, vol. 6, pp. 27433–27441, 2018.
[16] F. Guo, Z. Liu, G. Sa, and J. Tan, "A position error representation method for planar arrays," *IEEE Antennas Wireless Propag. Lett.*, vol. 19, no. 1, pp. 109–113, Jan. 2020.
[17] C. M. Schmid, S. Schuster, R. Feger, and A. Stelzer, "On the effects of calibration errors and mutual coupling on the beam pattern of an antenna array," *IEEE Trans. Antennas Propag.*, vol. 61, no. 8, pp. 4063–4072, Aug. 2013.
[18] X. S. Yang, "A new metaheuristic bat-inspired algorithm," in *Nature Inspired Cooperative Strategies for Optimization*. Berlin, Germany: Springer, 2010, pp. 65–74.
[19] T. Van Luyen and T. V. B. Giang, "Interference suppression of ULA antennas by phase-only control using bat algorithm," *IEEE Antennas Wireless Propag. Lett.*, vol. 16, pp. 3038–3042, 2017.
[20] Q. Yao and Y. Lu, "Efficient beamforming using bat algorithm," in *IEEE MTT-S Int. Microw. Symp. Dig.*, Beijing, China, Jul. 2016, pp. 1–2.
[21] L. van Tong and V. B. G. Truong, "BAT algorithm based beamformer for interference suppression by controlling the complex weight," *REV J. Electron. Commun.*, vol. 7, no. 4, pp. 87–93, 2018.
[22] X. Xiao and Y. Lu, "Data-based model for wide nulling problem in adaptive digital beamforming antenna array," *IEEE Antennas Wireless Propag. Lett.*, vol. 18, no. 11, pp. 2249–2253, Nov. 2019.

[23] Z. Shao, L. F. Qiu, and Y. Zhang, "Design of wideband differentially fed multilayer stacked patch antennas based on bat algorithm," *IEEE Antennas Wireless Propag. Lett.*, vol. 19, no. 7, pp. 1172–1176, Jul. 2020.
[24] Y. Xu, X. Shi, A. Wang, and J. Xu, "Design of sum and difference patterns with common nulls and low SLLs simultaneously in the presence of array errors," *IEEE Trans. Antennas Propag.*, vol. 67, no. 2, pp. 934–944, Feb. 2019.
[25] J. Li and P. Stocia, Eds., *Robust Adaptive Beamforming*. New York, NY, USA: Wiley, 2005.

ANYI WANG was born in Shandong, China, in 1968. He received the B.S. degree in communication engineering from the Xi'an Mining Institute (the Predecessor of the Xi'an University of Science and Technology), in 1992, the M.S. degree in electric drive and automation from the Xi'an Institute of Science and Technology (also the Predecessor of the Xi'an University of Science and Technology), in 1995, and the Ph.D. degree in signal and information processing from Xidian University, Xi'an, China, in 2001.

He is currently the Dean of the School of Communication and Information Engineering, Xi'an University of Science and Technology, the person in charge of Ph.D. degree in mining information engineering discipline and also a member of Shaanxi Provincial Standardization Expert Committee. Since 1995, he has been with the School of Communication and Information Engineering, Xi'an University of Science and Technology, an Assistant Professor, from 1995 to 1997, a Lecturer, from 1997 to 2003, an Associate Professor, from 2003 to 2009. He has been a Professor, since 2009. From 2001 to 2005, he worked as a Postdoctoral Fellow with Datang Mobile Communication Equipment Company Ltd.

He received the Third Prize of Science and Technology Progress Award of China Communications Society, the Second Prize of Science and Technology Progress Award of Shaanxi Province, and Xi'an Science and Technology Progress Award, in 2014, 2013, and 2015, respectively.

XUHONG LI was born in Xinjiang, China. She received the B.S. degree in industrial electric automation from the Xi'an Mining Institute, Xi'an, China, in 1994.

From 1994 to 1995, she works as an Electronics Engineer with the Yantai Dongfang Electronics Group. In 1995, she went to the School of Communication and Information Engineering, Xi'an University of Science and Technology, where she has been working as an Associate Professor. Her research interests include communication circuit and system technology, wireless communication, and industry application information technology.

YANHONG XU (Member, IEEE) was born in Shandong, China, in 1989. She received the B.S. degree in electronic engineering and the Ph.D. degree in electromagnetic field and microwave technology from Xidian University, Xi'an, China, in 2012 and 2017, respectively.

From January 2018 to December 2019, she works as a Lecturer with the School of Communication and Information Engineering, Xi'an University of Science and Technology, where she is working as an Associate Professor, since December 2019. From February 2018 to February 2020, she works as a Postdoctoral Fellow with the State Key Laboratory of Terahertz and Millimeter Waves, Department of Electrical Engineering, The City University of Hong Kong. Her research interests include array antenna theory and technology, low sidelobe pattern synthesis, array beamforming, wideband antenna design, and millimeter wave antenna technology.